Gas-Phase Vibrational Spectroscopy and Ab Initio Study of Organophosphorous Compounds: Discrimination between Species and Conformers

ARTICLE *in* THE JOURNAL OF PHYSICAL CHEMISTRY B · OCTOBER 2008

Impact Factor: 3.3 · DOI: 10.1021/jp804665h · Source: PubMed

7 AUTHORS, INCLUDING:

A. Cuisset
French National Centre for Scientific Resea…
48 PUBLICATIONS **252** CITATIONS
SEE PROFILE

G. Mouret
Université du Littoral Côte d'Opale (ULCO)
77 PUBLICATIONS **605** CITATIONS
SEE PROFILE

Olivier Pirali
SOLEIL synchrotron
110 PUBLICATIONS **581** CITATIONS
SEE PROFILE

Jean Demaison
Université des Sciences et Technologies de …
352 PUBLICATIONS **4,752** CITATIONS
SEE PROFILE

Chemical Physics Letters 492 (2010) 30–34

Contents lists available at ScienceDirect

Chemical Physics Letters

journal homepage: www.elsevier.com/locate/cplett

Far-infrared high resolution synchrotron FTIR spectroscopy of the ν_{11} bending vibrational fundamental transition of dimethylsulfoxyde

Arnaud Cuisset [a,*], Lia Nanobashvili [a,b], Irina Smirnova [a,c], Robin Bocquet [a], Francis Hindle [a], Gaël Mouret [a], Olivier Pirali [d,e], Pascale Roy [d], Dmitriĭ A. Sadovskiĭ [a]

[a] Laboratoire de Physico-Chimie de l'Atmosphère, UMR CNRS 8101, Université du Littoral – Côte d'Opale, 59140 Dunkerque, France
[b] Department of Exact and Natural Sciences, Graduate Program in Electrical and Electronic Engineering, Ivane Javakhishvili Tbilisi State University, Tbilisi, Georgia
[c] Physical Faculty of the M.V. Lomonosov Moscow State University, Moscow, Russia
[d] Synchrotron SOLEIL, L'orme des Merisiers, Saint-Aubin – BP48, 91192 Gif-sur-Yvette, France
[e] Laboratoire de Photophysique Moléculaire, CNRS, Bât. 210, Université Paris-Sud, 91405 Orsay Cedex, France

ARTICLE INFO

Article history:
Received 15 March 2010
In final form 16 April 2010
Available online 21 April 2010

ABSTRACT

We report the first successful high resolution gas phase study of the 'parallel' band of DMSO at 380 cm^{-1} associated with the ν_{11} bending vibrational mode. The spectrum was recorded with a resolution of 0.0015 cm^{-1} using the AILES beamline of the SOLEIL synchrotron source, the IFS 125 FTIR spectrometer and a multipass cell providing an optical path of 150 m. The rotational constants and centrifugal corrections obtained from the analysis of the resolved rotational transitions reproduce the spectrum to the experimental accuracy.

1. Introduction

Dimethylsulfoxyde (DMSO) is an excellent solvating agent which has many important applications in chemistry, biochemistry and industry. In the ocean atmosphere, DMSO is naturally emitted from the oxidation of dimethylsulfide (DMS) produced by the marine phytoplankton and plays a significant role in the atmospheric chemistry of sulfur [2]. Furthermore, DMSO is considered to be an organosulfide simulant of toxic agents such as mustard gas. In addition to its importance for industrial and environmental studies, the monitoring of DMSO concentrations is of considerable interest for civil protection.

The first spectroscopic analysis of the microwave (MW) transitions in the ground state of DMSO which allowed quartic centrifugal distortion constants to be determined, was reported in Refs. [4,3] and later again in Ref. [5]. Most comprehensively, up to $J = 50$, the ground state has been recently re-analyzed in Ref. [6]. The last reported experiments on gas phase rovibrational spectra of DMSO go back more 30 years [7] and were limited to low resolution and wavenumbers above 600 cm^{-1}. The harmonic force field of DMSO was determined by Typke and Dakkouri in 2000 [8] using liquid phase data for the low-frequency bending modes, and using vibrational satellite bands in the MW region for the torsional modes with predicted frequencies below 300 cm^{-1}.

In this context, the first gas phase high resolution Far-InfraRed (FIR) spectroscopic analysis of DMSO was undertaken recently in Ref. [9]. This work made full use of the exceptional properties of the AILES beamline of the SOLEIL synchrotron in the THz/FIR domain [10,11]. In the present Letter, we report on the first successful analysis of the gas phase rovibrational transitions involving one of the lowest frequency vibrational modes of DMSO.

DMSO is a 10-atom molecule with C_s symmetry, whose equilibrium configuration, calculated at the MP2/cc-pV(T+d)Z level of theory, is shown in Fig. 1. This average structure was derived by Typke and Dakkouri [8] after combining available data from IR, Raman and MW spectroscopy, and gas electron diffraction with *ab initio* predictions and reevaluating the harmonic force field of the molecule. Our preliminary experiments performed with the internal sources of the IFS125 Bruker FTIR spectrometer [12] allowed to update the experimental vibrational frequencies of all the IR active modes of DMSO (cf Fig. 2) and to obtain a better agreement with the force field developed in Ref. [8].

At low vibrational excitations, the two methyl groups of DMSO cannot rotate internally and the vibrations of the molecule can be analyzed in terms of 24 normal modes [8]. A number of these modes, notably the symmetric (A'-type) ν_{11} and the asymmetric (A''-type) ν_{23} related to the bending vibrations of the OSC_2 frame, have frequencies in the THz domain and are strongly dipole active. However, up until now, the rotational structure of these states could not be studied due to the very low vapor pressure of DMSO and low intensity of the conventional radiation sources in this frequency domain. The lowest frequency modes (201 and 219 cm^{-1} in Fig. 2) correspond to torsional vibrations of the two methyl groups.

* Corresponding author. Fax: +33 328237613.
E-mail addresses: Arnaud.Cuisset@univ-littoral.fr (A. Cuisset), sadovski@univ-littoral.fr (D.A. Sadovskiĭ).

0009-2614/$ - see front matter © 2010 Elsevier B.V. All rights reserved.
doi:10.1016/j.cplett.2010.04.042

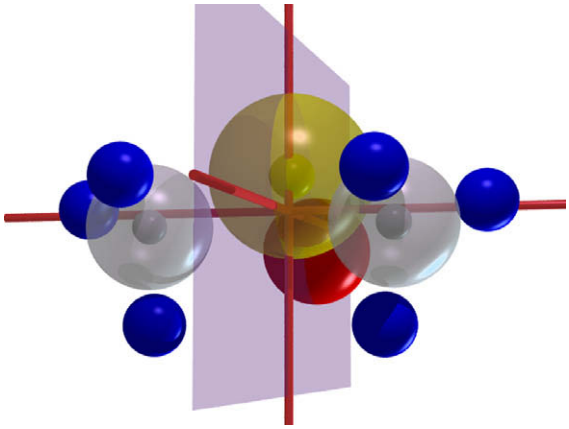

Fig. 1. Schematic representation of the equilibrium configuration of DMSO according to an *ab initio* calculation at the MP2/cc-pV (T + d) Z level of theory [1]; axes correspond to the three principal axes of inertia crossing at the center of mass, axes *B* and *C* (vertical) lie in the the symmetry plane.

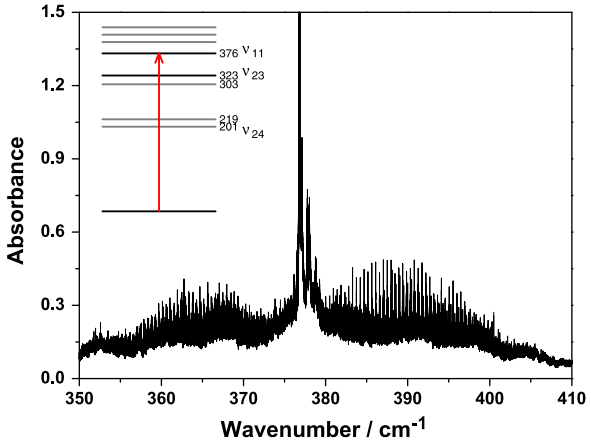

Fig. 2. Spectrum of the ν_{11} fundamental band of DMSO observed using the AILES beamline of the SOLEIL synchrotron ($P = 0.06$ Torr, $L = 150$ m, $\Delta\nu = 0.00015$ cm^{-1}, 700 scans, 46 h of acquisition). The rms noise in units of the Absorbance axis is estimated as ~0.028 at 350 cm^{-1} and ~0.014 at 410 cm^{-1}. The insert (top left) shows the system of the lowest vibrational energy levels of DMSO (frequencies in cm^{-1} are supplied next to the levels) according to our measurements and, for the two lowest modes, to [8]. Gray lines represent nearly dipole inactive states and their overtones, the arrow shows the ν_{11} transition observed in this work.

These modes are practically inactive in the absorption spectrum. However, their overtones and combination may play the role of 'dark states' perturbing $|\nu_{11} = 1\rangle$.

2. Experimental details

The high brilliance and the small divergence of the synchrotron radiation (SR) in the THz/FIR domain can reduce drastically the acquisition time of weakly absorbing high resolution rovibrational spectra [13]. Several synchrotron facilities, notably the Canadian Light Source, the Australian synchrotron, the SOLEIL synchrotron facility, and others have different IR beamlines used for high resolution spectroscopy [14,15].

The absorption spectra of DMSO have been recorded in the 20–600 cm^{-1} spectral range on the FIR beamline AILES of SOLEIL. Opened to external users at the end of 2008, AILES has already demonstrated its exceptional suitability for gas phase high resolution THz spectroscopy in a number of studies [16–18]. In our present study, the synchrotron radiation was essential in order to observe, in a limited time, the resolved rovibrational FIR spectrum of DMSO.

The AILES beamline was designed to obtain exceptional performances in terms of flux, spectral range, and stability over the entire IR domain. [10] have developed a reliable high resolution spectroscopic instrument providing high sensitivity over a wide frequency range [10]. Comparison with classical globar sources showed that the main gain from the use of the SR was obtained in the THz/FIR spectral domain. According to the recent comparative measurements in the 100 cm^{-1} region [11], the delivered flux and the achieved *S*/*N* ratio for the SR are factor of 40 higher than those of a conventional source, such as the mercury discharge lamp.

In our experiments, the SR was focused onto the entrance aperture of a high resolution Bruker IFS 125 Fourier transform interferometer containing a 6 μm mylar-silicon composite beamsplitter suitable for the THz spectral range. In order to limit the absorption due to the atmospheric compounds, the interferometer was continuously evacuated to 10^{-5} Torr. The detector was a helium-cooled silicon bolometer equipped with an optical band-pass filter having FWHM in the range of 10–600 cm^{-1}. DMSO with a purity better than 97% was obtained from Aldrich Chemical Co. and was used without further purification. The sample cell was filled by direct injection of the saturated vapor pressures at room temperature (0.42 Torr at 293 K). Due to the low volatility of the compound, a high sensitivity was required for these experiments. The spectrometer was coupled to a multipass cell (in a White type configuration) and adjusted to reach a 150 m optical path length. This cell was isolated from the interferometer by 50 μm thick polypropylene windows.

The observed spectrum associated with the ν_{11} rovibrational transition of DMSO is shown in Fig. 2. The spectrum was recorded with the resolution $\Delta\nu = 0.0015$ cm^{-1} at a pressure of 0.06 Torr. To achieve a *S*/*N* ratio > 100 in the ν_{11} region, we had to co-add the Fourier transforms of 700 interferograms. The total acquisition time amounted to 46 h. Note that with conventional sources, several months would be necessary to obtain a similar *S*/*N* ratio. The spectrum in Fig. 2 was calibrated using residual water absorption lines whose wavenumbers were taken from the HITRAN spectroscopic database [19]. The calibration accuracy was about 0.00015 cm^{-1} (RMS). For clarity, the residual water lines were subsequently removed manually from the spectrum presented in Fig. 2.

3. Specifics of the rotational structure of DMSO

DMSO is a slightly asymmetric top molecule with two nearly equal rotational constants $A \gtrsim B$, and significantly smaller third constant *C*. Its asymmetry parameter

$$\kappa = 1 - 2\varepsilon^2 = \frac{2B - (A + C)}{A - C} \approx 0.91, \quad (1)$$

is close to that of an *oblate* symmetric top ($\kappa = 1$). This specificity of DMSO was mentioned in Ref. [3] and the example of DMSO was used to discuss *K*-doubling and Watson's *S*-reduction [3,20,21].

Fig. 3 illustrates the classical rotational energy of DMSO in the ground state $|0\rangle$which is obtained after replacing the components $(J_a J_b J_c)$ of the angular momentum operator **J** for their classical analogs

$$(J_a, J_b, J_c) = \|\mathbf{J}\|\,(\cos\theta,\ \sin\theta\sin\phi,\ \sin\theta\cos\phi).$$

Here $\|\mathbf{J}\| = \sqrt{J(J+1)}$ is given by the quantum number *J*, and (θ, ϕ) define coordinates on the reduced rotational phase space $\mathbb{S}_J^2$. We can see that most of $\mathbb{S}_J^2$ is taken up by stable rotations about axis *C* which correlate to those in the oblate symmetric top limit (concentric stripes in Fig. 3). Rotations about axis *A* are represented by a much smaller domain of $\mathbb{S}_J^2$ (white area near axis J_a in the equato-

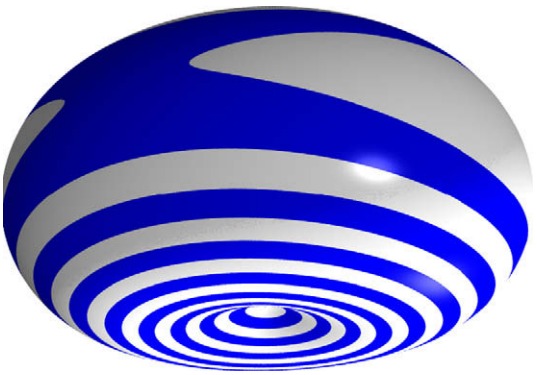

Fig. 3. Classical rotational energy of DMSO in the vibrational ground state $|0\rangle$ with $J = 25$. The energy (to a fixed constant) is given by the radial distance from the origin of the plot. The surface is drawn in slightly rotated coordinates (J_a,J_b,J_c) of Fig. 1. Equidistant levels of constant energy are stripe painted to display more clearly the shape of the surface. We see a deep minimum along the J_c axis (vertical) and a very shallow relief in the equatorial area with a small white maximal energy domain of stable classical rotation about axis J_a.

rial belt of the surface), and a similarly small domain (self-intersecting blue stripe in Fig. 3) corresponds to delocalized unstable motions with energies between those of the *C* and *A* rotations. To appreciate how close the molecule is to the symmetric top limit, imagine [22] switching the ^{16}O atom for its isotope ^{17}O or ^{18}O. In the usual DMS^{16}O (Fig. 1), axis *A*, or the stable principal axis with minimal moment of inertia, is the axis *perpendicular* to the symmetry plane. DMS^{17}O is very close to the symmetric top, and in DMS^{18}O axes *A* and *B* are interchanged, and the stable axis lies *in-plane*.

Given that (in the simplest rigid rotor approximation) the relative area of the *A*-domain of $\mathbb{S}_J^2$ is

$$\frac{2}{\pi}\arcsin\varepsilon = \frac{2}{\pi}\arcsin\sqrt{\frac{A-B}{A-C}} \approx 0.14,$$

the number of quantum states localized in that domain, or *A-states*, is below 10–15% of all states. Furthermore, since localized states form doublets, the number of the latter can be estimated as $\approx 0.14J$ and so they exist only for $J > 8$. The rest of the states are the *C*-states which correlate with the oblate symmetric top states and which are classified adequately by the good quantum number $K = K_c$ of J_c. For this reason, axis *C* is the most natural choice of the quantization axis for the rotational basis functions $|J,K\rangle$ used to construct the matrix of the effective rotational Hamiltonian $H(\mathbf{J})$.

Recall that to minimize the number of adjustable parameters in the rotational Hamiltonian, the latter is reduced to a D_2-symmetric form following the procedure by Watson [23]. This form is not unique and for nearly symmetric tops, it is customary [3,20,24,21] to use the *s*-form because it requires a smaller transformation and so is, in principle, a faster converging series. Additionally, one may also expect a lesser distortion of the original dipole moment operator. This all may be beneficial to the initial stages of the spectroscopic analysis and to higher *J* extrapolations.

In practice, however, the situation is less straightforward. In addition to a scalar series in J^2, the *s*-form Hamiltonian includes diagonal and tensorial terms. The former are various powers of K^2 (or $\cos^2\theta$) and contribute primarily to the energies of the *C*-states, while the latter also includes powers of $(J_a \pm iJ_b)^2$ (or $\sin^2\theta$) that describe the *A*-states or the intermediate states. The number of terms of each kind is roughly equal, while the number of *C* states is much larger. This disproportion may result in stronger correlations between the tensorial terms, especially when the *A*-states are observed with lower precision or not observed at all. In such cases, the *a*-form may turn out more stable [6].

4. Analysis of the ν_{11} fundamental

In our present analysis, we treated the $|\nu_{11} = 1\rangle$ fundamental as an isolated vibrational state, i.e., we considered no explicit Coriolis interactions with other close lying states, notably the $|\nu_{23} = 1\rangle$ fundamental, and no vibrational resonances, such as the Fermi reso-

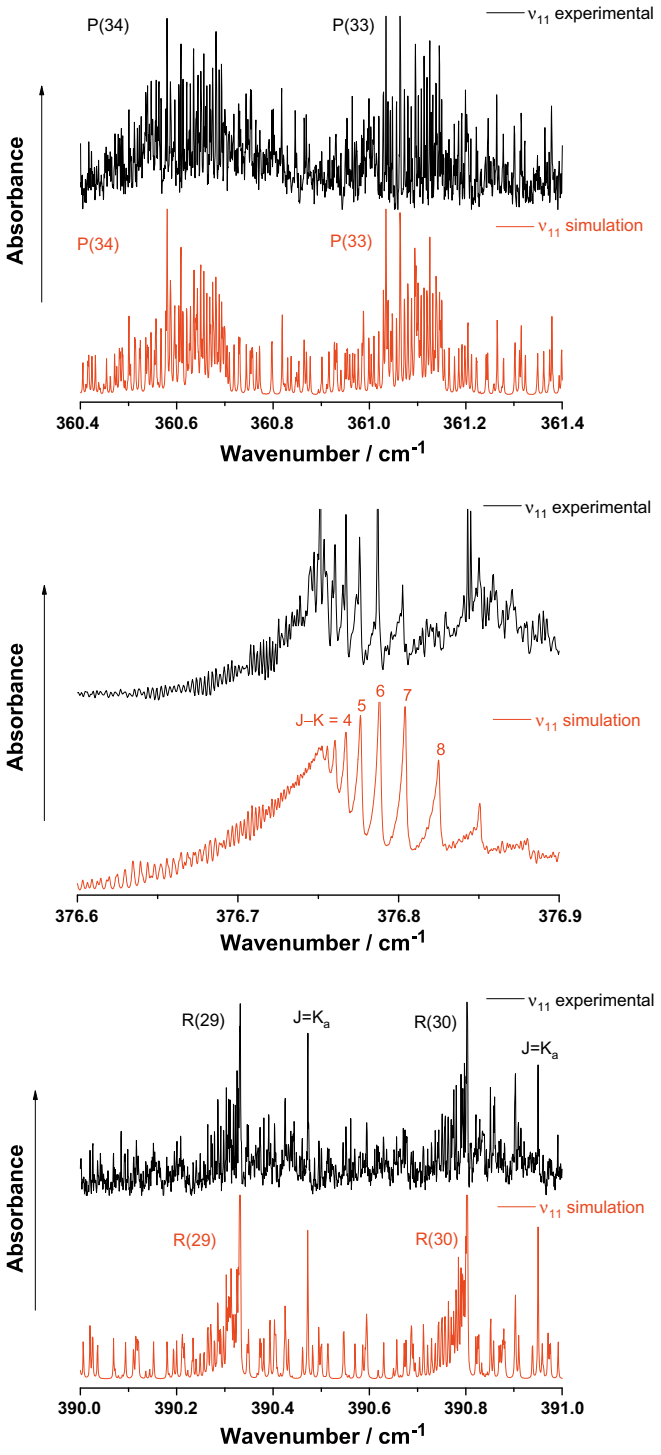

Fig. 4. Fragments of the observed and calculated spectra of the ν_{11} band of DMSO; top to bottom *P*-branch, *Q*-branch, and *R*-branch. The predicted spectra are simulated using the Lorentzian profile with HWHM of 0.0008 cm^{-1}. The unresolved *Q*-branch was not used in the fit, it is extrapolated using parameters in Table 1; the observed feature near 376.85 cm^{-1} belongs to a different band which was not analyzed in this work, see text.

nance with the $|v_{24}=2\rangle$ overtone (cf Fig. 2 and [8]). This turned out to be sufficient within the accuracy of our data and the range of the observed J values. In our approximation, the effective rovibrational Hamiltonian

$$H = \omega_{11}\, v + (A + v\delta A)J_x^2 + (B + v\delta B)J_y^2 + (C + v\delta C)J_z^2 + \cdots$$

includes purely rotational terms describing the ground state and their corrections in the upper state $|v=1\rangle$. For the higher order terms in H, we used Watson's s-form with axis z the axis C of the oblate symmetric top limit. As discussed in Section 3, such a choice is the most physical for DMSO. Moreover, we had the advantage of observing sufficient A-state transitions to stabilize the s-form in the least square fit.

The initial analysis and assignments became possible after observing that the $|0\rangle \rightarrow |v_{11}=1\rangle$ was quite similar to a parallel band of a symmetric top molecule: a strong Q-branch shouldered by weaker and reasonably regular P- and R-branches (see Fig. 2). This meant that out of the two components of the in-plane dipole moment $\mu(q) = (0,\mu_b,\mu_c)^T q$ induced by this A'-symmetric vibration, the C-component (that would be responsible for a parallel transition in the symmetric top) was stronger. Examing more closely the Fig. 4, the band had a complex, dense, and unresolved Q-branch, which extended far enough to obscure the low-J multiplets of the P-branch, while the beginning of the R-branch was buried under additional dense bands, possibly hot bands, off the high frequency head of the Q-branch. Nevertheless, entering basic rotational and dipole moment parameters, we managed to model several P- and R-branch $J = 12\ldots15$ multiplets well enough for picking combination frequencies and making unambiguous assignments. After that, fitting the spectrum became relatively straightforward. We used the programs by Pickett [25,26] for computing and fitting the spectra and the programs by Kisiel [27,28] to assist assignment.

Combining the MW $|0\rangle \rightarrow |0\rangle$ data from [6] and our FIR measurements on $|0\rangle \rightarrow |1\rangle$, we adjusted all parameters in H and reproduced the experimental data close to their estimated experimental accuracy, see Table 1 and Fig. 5. To this end it was necessary to develop H to degree 8 in (J,K). Fig. 5 shows that we have been able to reach all levels within assigned J-multiplet, and in particular levels of type A at the high energy end. The latter was possible due to the strong transitions to the topmost A-state doublet with $K_a = \pm J$ which could be observed very clearly at the blue edge of R multiplets, see Fig. 4.

The resulting parameter values are given in Table 1 and the measured transitions in the P and R branches of the band v_{11} are given as supplementary materials in Appendix A. Because the accuracy of the MW data was 0.03 MHz while that of the FIR data was about 5 MHz, the resulting $|0\rangle$ parameters were slightly affected by the FIR combination frequencies, and are close to those obtained in

Table 1
Parameters of the effective rotational Hamiltonian including purely rotational terms describing the ground state (left) and their corrections in the upper $|v_{11}=1\rangle$ state (right).[a] Also provided is the summary of the experimental data used for each state, the accuracy σ_{calc} of the fit, and the number of lines reproduced with errors outside the $2\sigma_{calc}$ interval.

$\|0\rangle$		$\|v_{11}=1\rangle$		
		ω_{11}	11294.71934 (72)	GHz
A	7036.58255 (19)	δA	5.0427(80)	MHz
B	6910.83024 (19)	δB	3.6235(81)	MHz
C	4218.77665 (27)	δC	−1.0061(68)	MHz
$-D_K$	−3.99040(47)	$-\delta D_K$	0.193 (29)	kHz
$-D_{JK}$	8.93877(55)	$-\delta D_{JK}$	−0.451(36)	kHz
$-D_J$	−6.08972(36)	$-\delta D_J$	0.299 (16)	kHz
d_1	−0.163670(63)	δd_1	0.066 (11)	kHz
d_2	−0.271802(33)	δd_2	0.0443(75)	kHz
H_K	−0.02233(50)	δH_K	0.044(39)	Hz
H_{JKK}	0.05486(70)	δH_{JKK}	−0.141(74)	Hz
H_{JJK}	−0.04143(56)	δH_{JJK}	0.196(57)	Hz
H_J	0.00946 (28)	δH_J	−0.089 (18)	Hz
h_1	−0.002260(72)	δh_1	−0.027 (14)	Hz
h_2	0.001283(70)	δh_2	−0.030 (13)	Hz
h_3	−0.001384 (23)	δh_3	−0.0060(39)	Hz
L_J	−0.000181(79)	δL_J	0.0293(67)	mHz
L_{JJK}	0.00089 (21)	δL_{JJK}	−0.122 (26)	mHz
L_{JK}	−0.00123(43)	δL_{JK}	0.244(48)	mHz
L_{KKJ}	0.00032(50)	δL_{KKJ}	−0.263(43)	mHz
L_K	0.00007 (25)	δL_K	0.108 (18)	mHz
l_1	0.000243(32)	δl_1	0.0123(58)	mHz
l_2	−0.000139(36)	δl_2	0.0161(59)	mHz
l_3	0.000034 (17)	δl_3	0.0048(30)	mHz
l_4	−0.0000059(35)	δl_4	−0.00060(49)	mHz
Lines	1717 MW 807 FIR freq. diff.	1581 FIR		
J	1 . . . 39	5 . . . 40		
σ_{exp}	0.03 MHz	0.00015 cm^{-1}		
σ_{calc}	0.03 MHz	0.00022 cm^{-1}		
$\mathcal{N}_{>2\sigma}$	101 MW	36FIR		

[a] Quantities in parentheses correspond to the diagonal elements of the covariance matrix expressed in the units of the two last significant digits of the parameter value.

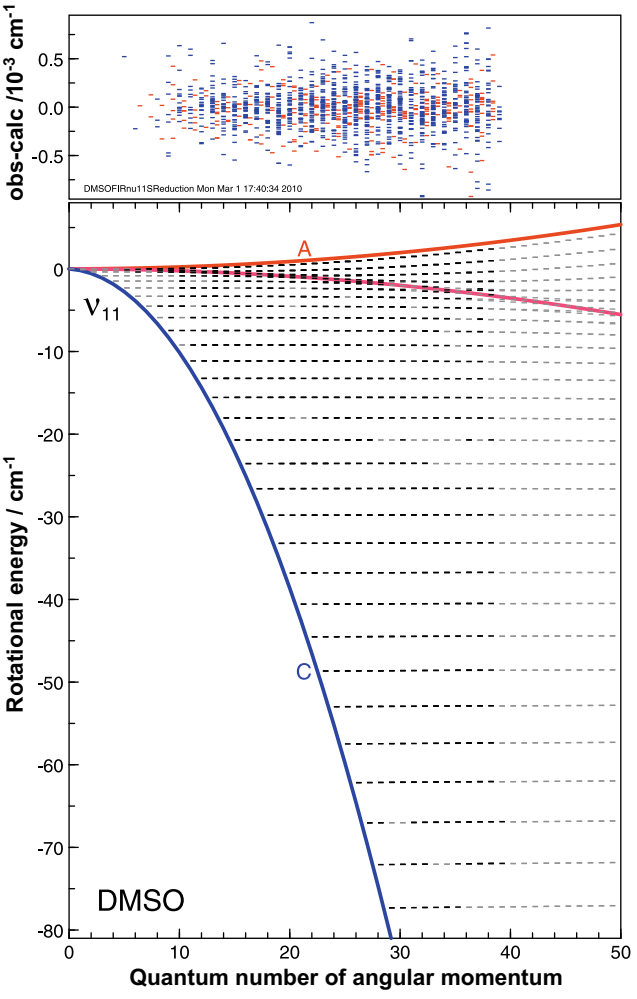

Fig. 5. Rotational energy levels (main panel) of DMSO in the vibrational state v_{11} according to parameters in Table 1. Energies are shown minus the scalar energy $H_s(J)$; bold solid lines represent energies of classical stationary axes of rotation (relative equilibria), observed levels are marked red. Small upper panel shows respective errors in reproducing rotational transitions in the v_{11} FIR band. Color version: red and blue represent A- and C-type levels, respectively. (For interpretation of the references to color in this figure legend, the reader is referred to the web version of the article).

Ref. [6] for their *S*-III choice. The intensities were described by a simple transition moment operator with a dominating *C*-component. We can see from Fig. 4 that they are in good overall qualitative agreement with the observed spectra. The intensity of the observed *Q*-branch band heads decreases more sharply than extrapolated from this simple model and furthermore, for $J - K \geqslant 7$ these heads are obscured by another band (see Section 5) which complicated further analysis.

We can see in Fig. 5 that the rotational structure of $|v_{11} = 1\rangle$ is standard. In fact, in the scale of the figure it differs invisibly from that of $|0\rangle$. There is no qualitative complications due to the closeness of the symmetric top limit. The only problem that we encountered was the persistent strong local perturbation of a single *C*-type $K = 15$ or 16 level in each multiplet starting with $J = 30$ (see gaps in Fig. 5). Additionally, we observed a small number of relatively weak and sparse lines that did not belong to our v_{11} band. The perturbed level sequence had to be excluded from our fit and its neighbors exhibited characteristically increasing systematic errors as they approached the perturber. These errors may have resulted in a slightly higher overall discrepancy of the fit compared to the estimated experimental uncertainty.

5. Conclusion

The existing high resolution gas phase spectroscopic data of DMSO only concerned the pure rotational transitions in the ground state. In the FIR domain, the low-frequency rovibrational transitions have never previously resolved. The high brightness of the SR and the instrumental sensitivity provided by the multipass cell allowed to measure for the first time these transitions. 1581 A-type and C-type transitions in the v_{11} band have been assigned and 25 molecular constants of Watson's s-form hamiltonian developed to degree 8 have been fitted within the experimental accuracy (see Table 1).

The use of the synchrotron radiation has opened many possibilities for new spectroscopic studies. Together with several other recent studies [16,18,17], our successful measurement and analysis of DMSO convincingly demonstrates the potential of the AILES beamline for high resolution FIR spectroscopy.

Thus our present work is just at the beginning of unraveling the rovibrational structure of low-frequency bending and torsional vibrational states of DMSO and yielding important comprehensive structural and spectroscopic information on this molecule. The next natural step in this study will be the analysis of the 'perpendicular' v_{23} band which was observed in the same experiment [9]. This analysis may be complicated by a possibly strong Coriolis interaction with another close vibrational state (303 cm^{-1}, see the scheme in Fig. 2).

It is also tempting to investigate further the nature of the perturbing state mentioned in Section 4. The little available information may suggest a 'dark' state situated within 15 cm^{-1} below $|v_{11} = 1\rangle$. From Fig. 2 and taking into account that harmonic frequencies [8] used to draw Fig. 2 are uncertain and anharmonic corrections may ran as high as 10–15 cm^{-1}, we may deduce that such a state may well be an $|v_{24} = 2\rangle$ overtone coupled to $|v_{11} = 1\rangle$ via a cubic Fermi term or q^3J Coriolis terms. Finally, in the same context, it is interesting to understand fully the origin of the other band (s) whose weaker *Q*-branch (es) is (are) observed in our experiment (see Fig. 4). Amongst different assumptions, the possibility of hot-band sequences involving the torsional levels populated at room temperature has to be considered. We anticipate substantial progress in answering these questions in the near future.

Acknowledgments

We thank B.I. Zhilinskií for discussions and encouragement and D. Balcon, J.B. Brubach and M. Rouzières of the AILES group at SOLEIL for their help during experiments; Lia Nanobashvili is grateful to LPCA and ULCO for financial support and assistance during her stay in France. We thank [6] for providing their MW data prior to the final publication of [6]. This work was partially funded by the Délégation Générale pour l'Armement (projet de Recherche Exploratoire et Innovation No. 06.34.037).

Appendix A. Supplementary data

Supplementary data associated with this article can be found, in the online version, at doi:10.1016/j.cplett.2010.04.042.

References

[1] M.J. Frisch et al., Computer Program GAUSSIAN 03, Rev. D.01, Gaussian, Inc., Wallingford, CT, 2004.
[2] O. Boucher et al., Atmos. Chem. Phys. 3 (2003) 49.
[3] V. Typke, J. Mol. Spectrosc. 63 (1976) 170 (See Table II on p. 174 for mw data on DMSO).
[4] W. Feder, H. Dreizler, H.D. Rudolph, V. Typke, Z. Naturforsch. A 24 (1969) 266.
[5] E. Fliege, H. Dreizler, V. Typke, Z. Naturforsch. A 38 (1983) 668.
[6] L. Margulès, R.A. Motiyenko, E.A. Alekseev, J. Demaison, J. Mol. Spectrosc. 260 (2010) 23.
[7] G. Geiseler, G. Hanschmann, J. Mol. Struct. 11 (1972) 283.
[8] V. Typke, M. Dakkouri, J. Mol. Struct. 599 (2001) 177.
[9] A. Cuisset et al., P. Roy, A.I.P Conf. Proc., vol. 1214, 2010, p. 85.
[10] P. Roy, M. Rouzières, Z. Qi, O. Chubar, Infr. Phys. Technol. 49 (2006) 139.
[11] J.B. Brubach et al., A.I.P Conf. Proc., vol. 1214, 2010, p. 81
[12] A. Cuisset, G. Mouret, O. Pirali, P. Roy, F. Cazier, H. Nouali, J. Demaison, J. Phys. Chem. B 112 (2008) 12516.
[13] A.R.W. McKellar, J. Mol. Spectrosc. 2010, in press, doi:10.1016/j.jms.2010.04.006.
[14] A.R.W. McKellar, B. Billinghurst, J. Mol. Spectrosc. 260 (2010) 66.
[15] T. Chimdi, E.G. Robertson, L. Puskar, C.D. Thompson, M.J. Tobin, D. McNaughton, Chem. Phys. Lett. 465 (2008) 203.
[16] V. Boudon, O. Pirali, P. Roy, J.-B. Brubach, L. Manceron, J. Vander Auwera, J. Quant. Spectrosc. Rad. Transf. 111 (2010) 1117.
[17] D. Jacquemart, L. Gomez, N. Lacome, J.Y. Mandin, O. Pirali, P. Roy, J. Quant. Spectrosc. Rad. Transf. 111 (2010) 1223.
[18] F. Kwabia Tchana, J.M. Flaud, W.J. Lafferty, L. Manceron, P. Roy, J. Quant. Spectrosc. Rad. Transf. 111 (2010) 1277.
[19] L.S. Rothman et al., J. Quant. Spectrosc. Rad. Transf. 110 (2009) 533.
[20] D. Papousek, M.R. Aliev, Molecular vibrational–rotational spectra, Studies in Phys. and Theor. Chem, vol. 17, Elsevier, Amsterdam, 1982 (For asymmetric top molecules see chapter III.17 on p. 160).
[21] V. Typke, J. Mol. Struct. 384 (1996) 35.
[22] B. Zhilinskií, private communication, 2010.
[23] J.K.G. Watson, in: J.R. Durig (Ed.), Vibrational Spectra and Structure, vol. 6, Elsevier, 1977, p. 1.
[24] M.R. Aliev, J.K.G. Watson, in: K.N. Rao (Ed.), Molecular Spectroscopy – Modern Research, vol. III, Academic Press, 1985, p. 1.
[25] H.M. Pickett, J. Mol. Spectrosc. 148 (1991) 371.
[26] H.M. Pickett, SPFIT/SPCAT programs for vibration–rotation spectra, 2007. For more information and examples see also <http://www.ph1.uni-koeln.de/cdms/pickett> and <http://info.ifpan.edu.pl/kisiel/asym/pickett/crib.htm>.
[27] Z. Kisiel, ASCP/SVIEW programs for graphical assignments of vibration–rotation spectra, 2009. For applications see [28].
[28] Z. Kisiel, L. Pszczólkowski, I.R. Medvedev, M. Winnewisser, F.C.D. Lucia, E. Herbst, J. Mol. Spectrosc. 233 (2005) 231.